This is to certify that the
thesis entitled

THE DEVELOPMENT OF A NUCLEIC ACID-BASED METHOD FOR ASSESSING THE AGE OF BLOODSTAINS

presented by

RACHEL LYNN AIKMAN

has been accepted towards fulfillment
of the requirements for the

M.S. degree in Forensic Science

Major Professor's Signature

3/19/10

Date

THE DEVELOPMENT OF A NUCLEIC ACID-BASED METHOD FOR ASSESSING THE AGE OF BLOODSTAINS

By

Rachel Lynn Aikman

A THESIS

Submitted to
Michigan State University
in partial fulfillment of the requirements
for the degree of

MASTERS OF SCIENCE

Forensic Science

2010

ABSTRACT

THE DEVELOPMENT OF A NUCLEIC ACID-BASED METHOD FOR ASSESSING THE AGE OF BLOODSTAINS

By

Rachel Lynn Aikman

The ability to determine exactly when a crime occurred would be of great benefit to investigators. A method to age biological evidence would also provide information regarding a variety of crimes. The potential of using RNA degradation as a tool for aging forensic biological evidence was investigated in the current study. A variety of mRNAs, tRNAs, and rRNA from bloodstains aged up to five years were assayed using real-time PCR to discern whether their quantities related to sample age. It was hypothesized that the RNAs would undergo differential degradation based on their structural and functional variability. 18S rRNA and valine tRNA displayed a non-linear relationship over 250 days. It is likely that the rRNA was relatively stable and that the tRNA was undergoing variable degradation throughout the period investigated. Negative results were obtained for β-actin, cyclophilin D, and GAPD mRNAs and serine and alanine tRNAs. While currently limited in its forensic utility, an aging method based on RNA degradation has the potential to establish probative value for a variety of biological evidence.

ACKNOWLEDGMENTS

I would like to gratefully acknowledge the supervision of Dr. David Foran throughout the course of my research. Without his help this thesis would not have been possible. I would also like to thank my committee members, Drs. Steven Dow and R. William Henry, for their assistance.

I received technical advice from many people during this project. I wish to acknowledge Dr. Jeff Landgraf at the MSU Research Technology Support Facility, Dr. Aaron Tarone at the University of Southern California, Dr. Ashley Heath at Sigma Custom Products, and Derek Najarian at Bio-Rad Laboratories for their help with my unusual data.

I thank the MSU Graduate School, the School of Criminal Justice, and the Biological Sciences Program for their financial assistance.

Finally, I am grateful to my fellow graduate students, friends, and most of all, my family for their support and endless encouragement during the past few years.

TABLE OF CONTENTS

LIST OF TABLES

LIST OF FIGURES

Images in this thesis are presented in color.

INTRODUCTION

Determining exactly when a crime occurred is often one of the most important aspects of a forensic investigation, since it impacts alibis, the witness pool, and other relevant information. In addition, temporal analysis of crime is important to law enforcement agencies seeking to establish patterns behind regional criminal activity. "Crime mapping" has been championed as a method to determine the most effective allocation of law enforcement resources. Such analyses identify trends within geographic locations, selection of victims, and times at which crime occurs (Eck et al., 2005). Despite its importance, however, temporal evidence is difficult to obtain, since many crimes do not leave a signature time trail (Ratcliffe, 2002). For example, the victim is often absent during a burglary. Unless a time-stamped video surveillance system is available to record the theft, all that is known is that the crime occurred while the victim was gone. This is especially problematic when a home or business is unattended for consecutive hours or days. Even a witness does not guarantee temporal accuracy; for instance, victims of an assault are susceptible to distorted or selective memories caused by the trauma (Ochberg, 2002).

Genetic Material as Evidence

Deoxyribonucleic acid (DNA) and ribonucleic acid (RNA) are found in all biological fluids. DNA is a valuable form of evidence that is currently used to identify an individual or link a suspect to a crime scene, and has been extracted from sources as diverse as contact lenses, cigarette butts, and bite marks in cheese (reviewed by Wickenheiser, 2002). RNA has had less forensic utility, but assays of RNA levels have increased the accuracy of insect age prediction and estimation of the postmortem interval

(PMI) (Tarone et al., 2007). These entomological assays highlight the potential of nucleic acids as temporal indicators; however, no method exists for aging other forensic biological evidence. A method to age bodily fluids would provide information regarding a variety of crimes. For example, blood left by a burglar would aid in timing when the break-in occurred. More importantly, determining time of stain deposition might establish whether evidence has probative value.

DNA is a relatively stable molecule that is able to withstand both time and extreme environmental stress (Kobilinsky, 1992; Weedn and Roby, 1993). For instance, DNA has been successfully extracted from deflagrated pipe bombs and from bones as old as 30,000 years (Foran et al., 2009; Hofreiter et al., 2001, respectively). This stability means that DNA is not particularly useful as a temporal marker. On the other hand, RNA is less stable (Wang and Kool, 1995), and thus has the potential to provide forensically-relevant temporal information to an investigation. Different types of RNA molecules, including messenger RNA (mRNA), transfer RNA (tRNA), and ribosomal RNA (rRNA) have varying stabilities resulting from their unique cellular functions. Abelson et al. (1974) radioactively labeled total cellular mRNA, tRNA, and rRNA in resting and growing cells in order to compare their turnover. In both cellular states, they found that mRNA half-life was 9 hours, tRNA half-life was 36 hours, and 18S rRNA half-life was 72 hours. Based on these findings, if rates of decay were established for RNA targets, it may be possible to correlate their relative quantities in biological samples with the aging process.

Structural and Functional Differences in RNA Molecules

Messenger RNA

During transcription, an RNA polymerase is directed to a gene and a complementary mRNA molecule is synthesized (Figure 1). The transcript is then both enzymatically and chemically modified in order to remove non-coding sequences and promote protein production. On the 5' end, a methylated guanine nucleotide "cap" is added in order to recruit the protein-building machinery, the ribosome, to the mRNA. In addition, the 3' end is polyadenylated, which improves translational efficiency (Wilusz et al., 2001).

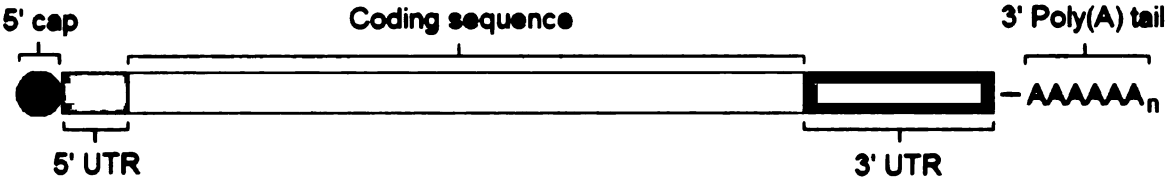

Figure 1: The structure of an mRNA molecule, including the 5' methyl-guanine cap, the 5' untranslated region (UTR), the protein coding sequence, the 3' UTR, and the 3' poly(A) tail.

Cellular degradation pathways for mRNA can be simplified into three basic steps: removal of the poly(A) tail, cleavage of the 5' cap, and degradation from the 5' end (Houseley and Tollervey, 2009). *In vivo*, this response can be both positively and negatively impacted by a variety of stimuli. For example, Herruer et al. (1988) reported that a temperature shift from 23 to 36°C caused a rapid, 85% decline in yeast ribosomal protein mRNAs. mRNA degradation has also been shown to be inhibited when yeast cells were subjected to starvation or osmotic stress (Jona et al., 2000; Greatrix and van Vuuren, 2006). In HeLa cells, exposure to ultraviolet light stabilized mRNA by preventing poly(A) tail removal (Gowrishankar et al., 2005). In addition, Sahmi et al.

(2006) found that mRNA levels in bovine ovarian cells were under direct hormonal regulation.

In human cells, mRNA stability controls protein production for 5 to 10% of genes (reviewed by Bolognani and Perrone-Bizzozero, 2008). The average half-life for a mammalian mRNA is 7 hours, although it may be less than an hour for regulatory protein mRNAs (such as transcription factors) or over 24 hours for those important in structure and metabolism (e.g. cytoskeletal and housekeeping proteins) (Sharova et al., 2009).

Transfer RNA

Transfer RNAs act as carriers for amino acids during protein production. All tRNA molecules display a cloverleaf shape and contain five main "loops" (Figure 2). The anticodon loop base-pairs with a specific three-base sequence on an mRNA, the codon. On the opposite side of the molecule is an acceptor arm that binds an amino acid. The other loops in the tRNA are responsible for stabilizing the three-dimensional L-shaped structure of the molecule (de Pouplana and Schimmel, 2001).

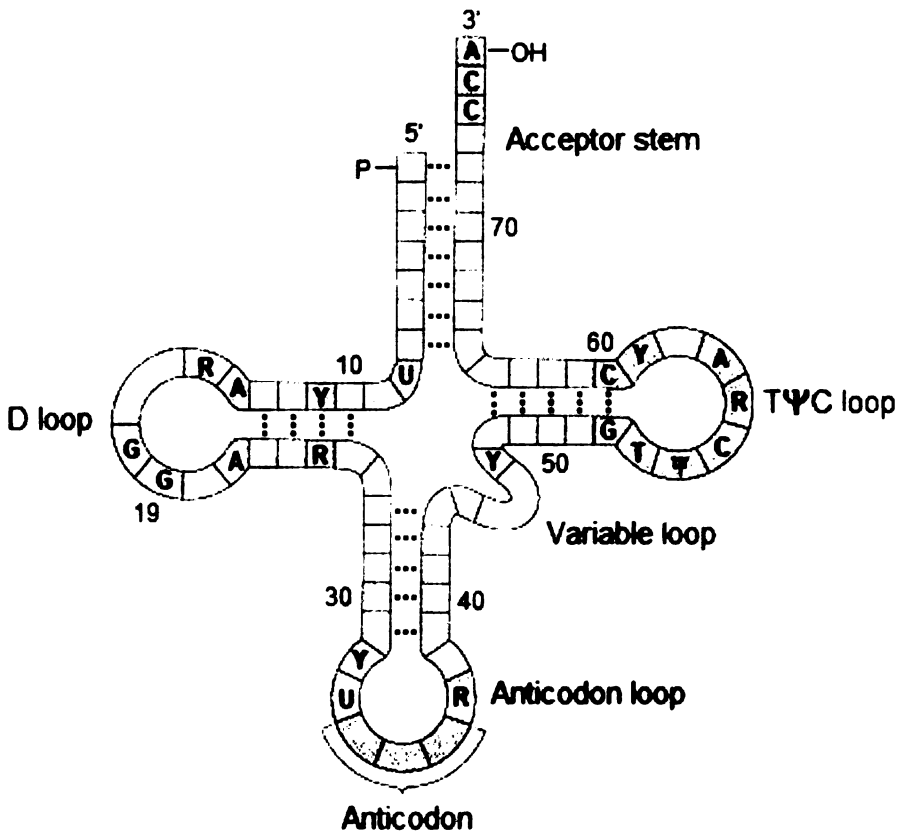

Figure 2: The general structure of a tRNA molecule, including the acceptor arm, anticodon loop, and anticodon. Figure is from Mathews et al. (2000).

tRNAs are relatively stable molecules due to their three-dimensional structure (Puglisi et al, 2003). In addition, post-transcriptional modifications to their nucleotides aid in their integrity (Engelke and Hopper, 2006). Yeast mutants lacking enzymes necessary to catalyze such modifications displayed cellular growth defects and tRNA half-lives similar to those of mRNAs (Alexandrov et al., 2006). Half lives differ greatly among tissues and are impacted by growth and development (Johnson et al., 1974). In mammalian cells, tRNA turnover ranges from 36 to 120 hours (Schlegel et al., 1978). While pathways responsible for tRNA degradation are still largely uncharacterized, data suggest that multiple independent pathways are involved in this regulation (Kadaba et al., 2004; Alexandrov et al., 2006).

Ribosomal RNA

The final step of protein production occurs in the ribosome, which consists of two subunits that assemble on an mRNA (Figure 3). These scan along the transcript in a 5' to 3' direction until a start codon is reached, at which point the peptidyl-transferase reactions involving tRNAs are initiated. rRNA plays a key role during this process, since it binds both the codon of the mRNA and the anticodon of the tRNA (Graifer et al., 2004).

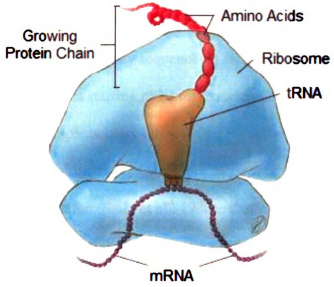

Figure 3: The ribosome assembled on an mRNA. rRNA is not depicted; however it is the component of the ribosome that physically links the mRNA and tRNA molecules. Figure is adapted from Davis (2005).

rRNAs are stable molecules, since they are shielded within a large complex consisting of the ribosomal subunits and a variety of additional binding proteins, initiation factors, and elongation factors (Merryman et al., 1999). It has been hypothesized that regions of these proteins that extend into the core stabilize the rRNAs by protecting their negatively-charged backbones (reviewed by Noller, 1991). rRNAs are perhaps most vulnerable to

degradation directly after their synthesis, prior to the formation of the ribosomal complex. However, in a study of yeast rRNA, Deshmukh et al. (1993) found that ribosomal protein-RNA interactions following rRNA synthesis provided at least some level of protection even in the absence of ribosomal assembly.

The Polymerase Chain Reaction

Nucleic acids can be quantified using a variation of the polymerase chain reaction (PCR). In its most basic form, PCR is a technique that targets a specific region of DNA and exponentially replicates it (Figure 4). First, the double-stranded DNA is heated and separated into single strands. Then, two short oligonucleotide primers, included in the reaction, anneal to their complementary sequence on either side of the DNA to be replicated. The primers act as a starting point for extension by a DNA polymerase during the third step, where the complementary DNA strand is synthesized. This process is repeated multiple times, resulting in the creation of billions of copies of the target sequence during a single reaction (Saiki et al., 1988). During PCR, there are three phases that occur based on the kinetics of the reaction (Bloch, 1991). In the exponential phase, product formation is highly favorable and the amount of product is doubled each cycle. The linear phase occurs when reagents limit the reaction and rate of synthesis slows. Finally, amplification stops completely and a plateau is reached. With standard PCR, products are detected following the plateau phase. As a result, the final amount of product is not directly related to the initial DNA concentration.

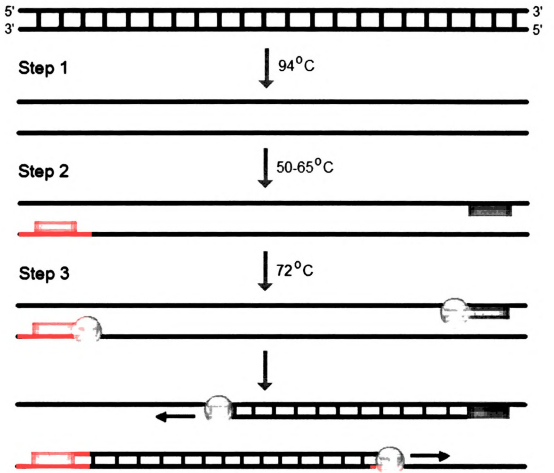

Figure 4: The three-step process of PCR. In the first step the DNA is heated and separated into two single strands. In the second step, the temperature is lowered and oligonucleotide primers anneal to either side of the desired DNA sequence. In the third step, a DNA polymerase binds to the primers and synthesizes the complementary DNA strands.

Measuring PCR product formation during the exponential phase allows the reaction to be used quantitatively. Most variations of quantitative PCR capture fluorescence that is produced as DNA product concentration increases. Real-time PCR using TaqMan® chemistry (Applied Biosystems) is one such technique (Figure 5). In this method, an oligonucleotide probe containing two fluorescent dyes is added to the reaction. Following each cycle, the first dye is excited by a laser and fluorescence is measured. In an intact probe the two dyes are in close proximity and the second quenches the

fluorescence from the first. As the DNA polymerase synthesizes a complementary strand during the extension step, it cleaves the probe and causes the dyes to be released, allowing the first dye's fluorescence to be measured (Holland et al., 1991). This process is repeated during each cycle of the reaction; the earlier the increase in fluorescence occurs, the greater the initial DNA concentration.

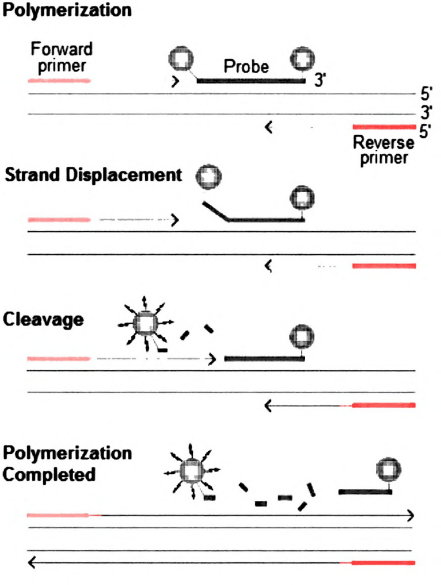

Figure 5: The TaqMan® real-time PCR reaction. Figure is adapted from Applied Biosystems TaqMan® Gene Expression Assays document (2006).

Real-time PCR amplification curves plot relative fluorescence units (RFU) at each cycle of the reaction (Figure 6). There is always some level of background fluorescence; therefore, a threshold fluorescence level is set above it during the exponential phase, which remains consistent among replicates. A threshold cycle (C_T) value is determined from the intersection of an amplification curve and the threshold: a lower C_T value indicates a greater amount of starting DNA (Heid et al., 1996). Sample DNA quantities can be directly compared to a standard containing a known amount of starting DNA, or they can be relatively compared to one another.

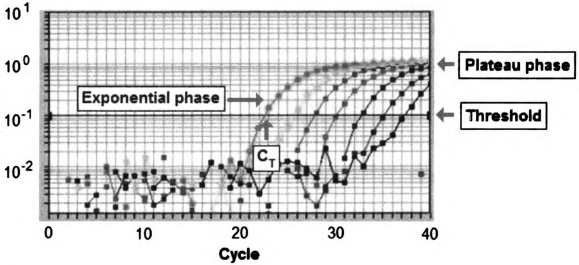

Figure 6: A series of real-time PCR amplification curves depicting the exponential and plateau phases. The threshold is represented as a horizontal line, and the C_T value for the leftmost curve is indicated. Figure is adapted from ABI PRISM 7700 (TaqMan® assay) Amplification Curve (2009).

PCR only amplifies DNA, so an additional step is required to quantify levels of RNA in a biological sample. The enzyme reverse transcriptase uses single-stranded RNA as a template to produce a complementary DNA molecule (cDNA) (Temin and Mizutani,

1970). When RNA is reverse-transcribed, the resulting cDNA represents all of the RNA from the sample and should retain the relative quantities of the different RNAs that are present. As a result, the combination of reverse transcription and real-time PCR is a powerful tool for quantifying RNA in biological samples.

Previous Research Involving RNA Degradation in Biological Samples

Preliminary research has been conducted to investigate whether RNA decay is a feasible age indicator for biological samples. Bauer et al. (2003) examined two methods for measuring RNA degradation in bloodstains: semi-quantitative duplex PCR and competitive PCR. First, two regions of β-actin were amplified from opposite ends of the cDNA. The authors hypothesized that PCR product near the 5' end of the cDNA would be more prevalent in reactions containing partially-degraded mRNA, because mRNAs are degraded from the 5' end (corresponding to the 3' end of the cDNA). In the second method, cyclophilin cDNA was amplified with a competitor: a molecule created from the same cDNA that was engineered to contain a small deletion, making size differentiation between the two products possible. The competitor was then added in known concentration to the PCR reaction. The premise was that the cDNAs would compete for use of the primers, and that the primers would act as a limiting reagent in the reaction (Zimmermann and Mannhalter, 1996). It was hypothesized that competitor cDNA should be present in a greater proportion when cyclophilin mRNA was more severely degraded.

The authors calculated PCR product ratios for each of the above methods: one for the 5' and 3' regions of β-actin and another for competitor versus endogenous cyclophilin. Ratios for both β-actin and cyclophilin mRNAs significantly increased over a period of 180 months ($p<0.05$), with older bloodstains displaying greater variability. Only blood

samples with age differences of greater than 4 years could be differentiated with statistical significance ($p<0.05$). Overall, the data show that it is possible to detect RNA degradation in aged bloodstains, and that the degradation is associated with sample age. However, the lack of precision limits the application of such methods, and indicates that semi-quantitative duplex PCR and competitive PCR are not ideal methods for RNA quantification.

More recently, Anderson et al. (2005) employed real-time PCR to quantify the levels of two common RNAs in bloodstains aged over 150 days. The researchers investigated whether degradation rates differed between the molecules and if their ratio could be used as a predictor of bloodstain age. C_T ratios of 18S rRNA to β-actin mRNA were calculated, which displayed a positive linear trend with age. Since a low C_T value corresponds to a greater amount of initial cDNA, an increase in the proportion of 18S to β-actin indicated that 18S was degrading at a more rapid rate than β-actin. However, the authors incorrectly stated that β-actin was less stable and decayed more rapidly than 18S. It was apparent that they misinterpreted a low C_T value as a low cDNA concentration, which inverted the results. The data were also inconsistent with previous work that showed 18S possessing greater stability than mRNA *in vivo* (Abelson et al., 1974). Due to the errors present in the study, conclusions could not be drawn regarding the stability of the individual RNAs. However, the data did indicate that RNA undergoes differential degradation and that relationships among molecules may be useful as indicators of age in biological samples. In addition, the results were obtained with small volumes of blood, demonstrating that the method would be viable with quantities of biological samples commonly found at a crime scene.

Current Work Aging Bloodstains Using RNA Degradation

The aim of the research presented here was to investigate the potential of RNA degradation as a tool for aging forensic biological evidence. Real-time PCR was used in an attempt to quantify a variety of mRNAs, tRNAs, and rRNA, and bloodstains aged up to five years were examined to discern whether quantities of the RNAs were related to sample age. It was hypothesized that the RNAs would undergo differential degradation based on their structural and functional variability. If relationships between molecules could be determined, a method for quantification of RNA degradation would have the potential to aid investigators in establishing temporal identities for biological evidence.

METHODS

Blood Sample Collection

Blood samples were provided by a volunteer, including fresh blood and stains approaching 5 years old. A region of the finger was cleaned with 70% ethanol and a lancet was used to draw blood. Multiple blood spots were dotted onto sterile plastic petri dishes, which were allowed to dry and stored at room temperature, protected from light. Additional blood samples were collected over the course of the research in the same manner. Ten were used for analysis, including a control of fresh blood that was not allowed to dry prior to RNA extraction. The dates of sample collection ranged from 10/22/03 to 5/8/08.

Selection of RNA Targets

The mRNA targets analyzed were housekeeping genes. Two of these, β-actin and cyclophilin D, had been used in previous research involving bloodstain aging (Bauer et al., 2003; Anderson et al. 2005). The third was glyceraldehyde-3-phosphate dehydrogenase (GAPD), another commonly-used RNA standard (Morse et al., 2005). Primer sequences for β-actin were taken from Bauer et al. (2003), those for cyclophilin D were from Medhurst et al. (2000), and the GAPD primers were developed by Carraro et al. (2005) (Table 1). The TaqMan® probe sequence for cyclophilin D was from Medhurst et al. (2000). The probes for β-actin and GAPD were designed by hand due to difficulties encountered using primer design software on short sequences. Probes were labeled with a hexachloro-6-carboxyfluorescein (HEX) reporter dye and black hole quencher (BHQ1) (Table 2). The oligonucleotides were designed for the human variant of the mRNAs.

The tRNAs assayed were alanine tRNA ($tRNA^{Ala}$), serine tRNA ($tRNA^{Ser}$), and valine tRNA ($tRNA^{Val}$). Oligonucleotides for the tRNAs were designed by hand, attempting to maximize sequence length and avoid hairpin structure (Figure 7; Table 1). TaqMan® probes were chosen based on the anticodons that are most prevalent in humans (Ikemura, 1985), including $tRNA^{Ala}$ (GGC), $tRNA^{Ser}$ (GCU), and $tRNA^{Val}$ (CAC). The corresponding probes were labeled with a tetrachloro-6-carboxyfluorescein (TET) reporter dye and black hole quencher (Table 2).

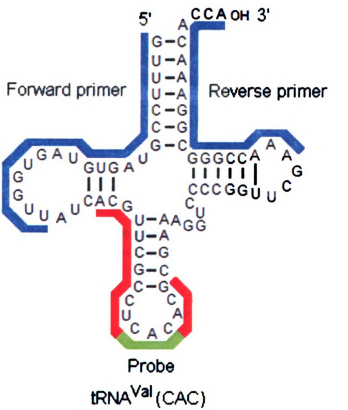

Figure 7: The location of the custom primers and probes designed for the tRNA molecules. $tRNA^{Val}$ (CAC) is pictured, however the same locations were used for $tRNA^{Ala}$ (GGC) and $tRNA^{Ser}$ (GCU). Figure is adapted from Achsel and Gross (1993).

The 18S rRNA molecule, which is part of the small ribosomal subunit, was also assayed. Primer sequences were from Niki et al. (2000) (Table 1). The probe was designed by hand and was labeled with a 6-carboxyfluorescein (FAM) reporter dye and black hole quencher (Table 2).

Table 1: Primer sequences and amplicon sizes for the RNA targets of interest.

Gene	**Primer Sequences 5'→3'**		**Size of Amplicon**
	Forward	**Reverse**	
β-actin mRNA	atccacgaaactaccttcaactc	gaggagcaatgatcttgatcttc	178 bp
Cyclophilin D mRNA	tgagacagcagatagagccaagc	tccctgccaatttgacatcttc	93 bp
GAPD mRNA	ctctctgctcctcctgttcgac	tgagcgatgtggctcggct	213 bp
$tRNA^{Ala}$ (GGC)	ggggctatagctcagctggg	agctatgcgggatcgaaccg	70 bp
$tRNA^{Ser}$ (GCU)	gtagtcgtggccgagtggtt	tggcgtagtcggcaggattc	85 bp
$tRNA^{Val}$ (CAC)	gtttccgtagtgtagtggtt	tggtgtttccgcccggttt	76 bp
18S rRNA	cggctaccacatccaaggaa	gctggaattaccgcggct	187 bp

Table 2: TaqMan® probe sequences and fluorophores for the RNA targets of interest.

Gene	Probe Sequence 5'→3'	Reporter Fluorophore	Quencher Fluorophore
β-actin mRNA	ctgtacgccaacacagtgct	HEX	BHQ1
Cyclophilin D mRNA	aacctatagctttaagctgtgtactgaatattggtgct	HEX	BHQ1
GAPD mRNA	gccgcatcttcttttgcgtc	HEX	BHQ1
$tRNA^{Ala}$ (GGC)	agcgcctgcttggcacg	TET	BHQ1
$tRNA^{Ser}$ (GCU)	ggcgatggactgctaatcc	TET	BHQ1
$tRNA^{Val}$ (CAC)	acgttcgcctcacacgc	TET	BHQ1
18S rRNA	taacgaggatccattggaggg	FAM	BHQ1

Isolation of RNA

Pipettors, disposable pipet tips, scalpels, tubes, and appropriate solutions were UV-irradiated for 6 minutes using a Spectrolinker UV Crosslinker (Spectroline) prior to use. The laboratory bench and pipettors were regularly treated with RNase*Zap* (Applied Biosystems), and all water was diethylpyrocarbonate (DEPC)-treated. RNA was first isolated using a guanidinium thiocyanate-phenol-chloroform extraction and TRIzol® reagent (Invitrogen). Twenty microliters of fresh blood was deposited into two microcentrifuge tubes. One milliliter of water was added and incubated at room temperature for 20 minutes. The tubes were centrifuged at maximum speed for 2 minutes and the supernatant was removed. One milliliter of TRIzol® reagent was added and a reagent blank was initiated and carried through the remainder of the procedure. Cells

were lysed by repetitive pipetting with a P1000 pipettor and centrifuged for 10 minutes at 12,000 x g at 4°C. The homogenates were transferred to new tubes, and the centrifugation and transfer repeated. Samples were incubated at room temperature for 5 minutes. Two hundred microliters of chloroform was added, and tubes were inverted to mix. They were incubated at room temperature for 5 minutes and centrifuged at 12,000 x g for 15 minutes at 4°C. The upper aqueous phases were transferred to new tubes, and 0.5 mL of RNase-free isopropanol was added. The precipitates were incubated at room temperature for 10 minutes and centrifuged at 12,000 x g for 10 minutes at 4°C. The supernatants were discarded and the RNA pellets were washed with 1 mL of 75% ethanol. The tubes were centrifuged at 12,000 x g for 5 minutes at 4°C, and the ethanol wash step was repeated twice more. The supernatants were removed, and the RNA pellets were vacuum-dried for 20 minutes and resuspended in 60 μL of water. This procedure was subsequently repeated on the aged bloodstain collection. The samples were scraped from petri dishes using a scalpel and the blood powder was placed into a microcentrifuge tube. TRIzol® reagent was directly added to the tube and the remainder of the procedure was as detailed above.

A second version of the TRIzol® procedure was also performed on the aged bloodstains. Blood samples were collected using a scalpel as described above and 1 mL of TRIzol® reagent was added to each tube, which were mixed and incubated at room temperature for 5 minutes. Two hundred microliters of chloroform was added and incubated at room temperature for 3 minutes. The tubes were centrifuged at maximum speed for 30 minutes at 4°C, and the upper aqueous phases were transferred to new tubes. Two hundred and fifty microliters of RNase-free isopropanol was added and incubated at

room temperature for 10 minutes. The tubes were centrifuged at maximum speed for 30 minutes at 4°C. The supernatants were removed and the RNA pellets were washed with 1 mL of 75% ethanol. The tubes were centrifuged at maximum speed for 15 minutes at 4°C and the supernatants were removed. The RNA pellets were air-dried in a laminar-flow hood for 10 minutes and resuspended in 56 µL of water.

A third RNA extraction method utilized a Qiagen QIAamp® RNA Blood Mini Kit. The protocol was first performed on one of the aged blood samples. Five variations of the resuspension step were performed to determine an optimal procedure. One blood sample was collected as a powder using a scalpel and placed in a microcentrifuge tube. One hundred microliters of Buffer EL was added. For the four remaining extractions, 500 µL of Buffer EL was added directly to the petri dish, and the blood was resuspended into the solution. Blood solution and Buffer EL were added to separate tubes in the following volumes (in µL): 5:5, 20:10, 100:50, and 250:125. The rest of the procedure followed the kit protocol. The tubes were incubated on ice for 15 minutes, being briefly vortexed twice during the incubation. They were centrifuged at 400 x g for 10 minutes at 4°C and the supernatants were removed. A volume of Buffer EL equivalent to that used in the first step was added, and cells were resuspended by vortexing. Centrifugation was performed at 400 x g for 10 minutes at 4°C and the supernatants were removed. Three hundred and fifty microliters of Buffer RLT was added and the tubes were vortexed. The lysates were added directly to QIAshredder® spin columns and centrifuged at maximum speed for 2 minutes. Three hundred and fifty microliters of 70% ethanol was added and mixed by repetitive pipetting with a P1000 pipettor. The lysates were transferred to QIAamp® spin columns and centrifuged for 15 seconds at 8,000 x g. The columns were

placed in new collection tubes and 700 µL of Buffer RW1 was added. The samples were centrifuged for 15 seconds at 8,000 x g, and the columns were transferred to new collection tubes. Five hundred microliters of Buffer RPE was added, and the tubes were centrifuged at 8,000 x g for 15 seconds. An additional 500 µL of Buffer RPE was added to each column, which were centrifuged at maximum speed for 3 minutes. Columns were placed in new collection tubes and were centrifuged at full speed for 1 minute. The spin columns were transferred to new microcentrifuge tubes and 50 µL of water was pipetted onto the QIAamp® membranes. The tubes were centrifuged at 8,000 x g for 1 minute. Variations of this procedure included using fresh blood samples that were briefly allowed to dry on petri dishes and various volumes of fresh blood (up to 1 mL) that were directly added to microcentrifuge tubes. Variables included blood volume, buffer volume, and incubation times. Reagent blanks were included in all procedures.

Portions of the RNA extractions were quantified with a Beckman DU 520 general purpose UV/VIS single-cell Spectrophotometer with 1 µL of RNA diluted with 199 µL of distilled water. Purity was calculated by the absorbance at 260 nm divided by the absorbance at 280 nm.

DNase I Treatment

Two DNase treatments were used on the RNA samples. In the first, 7 µL of DNase I and 7 µL of DNase I buffer were added to 40 µL of RNA and incubated at 37°C for 1 hour. The enzyme was heat-inactivated for 10 minutes at 75°C. One hundred microliters of isopropanol was added, and the samples were centrifuged at maximum speed for 30 minutes at 4°C. The supernatants were removed and the RNA pellets were washed with 60 µL of 70% ethanol. Tubes were centrifuged at maximum speed for 30 minutes at 4°C

and the supernatants were removed. The pellets were vacuum-dried for 15 minutes and resuspended in 32 μL of water. RNAs were stored at -80°C. The second treatment followed the one above, except 0.7 μL of 0.5 M ethylenediaminetetraacetic acid (EDTA) was added after the incubation. The enzyme was heat-inactivated at 75°C for 10 minutes, and RNAs were stored at -80°C.

Reverse Transcription

RNAs were reverse-transcribed using an Applied Biosystems High Capacity cDNA Archive Kit following the manufacturer's protocol. Sample volumes differed among RNA preparations, but the general proportions for the 2X reaction mix were:

10 μL 10X Reverse Transcription (RT) Buffer
4 μL 25X dNTPs
10 μL 10X random hexamer primers
5 μL MultiScribe™ Reverse Transcriptase (50 U/μL)
21 μL sterile, RNase-free water
50 μL total 2X reaction mix

The mix was diluted to 1X using an equal volume of RNA. In addition, a control lacking reverse transcriptase was prepared for each sample. Reactions were incubated at 25°C for 10 minutes and at 37°C for 2 hours. cDNAs were stored at -20°C.

PCR

Primers were optimized using standard PCR and control human DNA. Forward and reverse primers were tested in combinations of 0.9, 0.3, and 0.05 μM. A negative control included no DNA and the 18S primers. The reaction consisted of 1 μL of human DNA (10 ng/μL), 1 μL of the forward and reverse primers, 1 μL of dNTPs (2 mM), 1 μL of 10X PCR Buffer, 1 μL of bovine serum albumin (BSA) (1 μg/μL), 1 unit of Taq polymerase and 3.8 μL of water. The PCR samples were incubated at 95°C for 5

minutes, followed by 40 cycles of 95°C for 30 seconds, 55°C for 45 seconds, and 72°C for 1 minute. They remained at 72°C for an additional 5 minutes and were held at 4°C. In reactions where non-specific products were produced, the annealing temperature was increased to between 56 and 60°C. The PCR products were electrophoresed on a 4% agarose gel and stained with ethidium bromide. This same procedure was repeated using cDNA templates and controls consisting of a reagent blank, samples lacking reverse transcriptase, and human DNA with 18S primers.

Real-Time PCR

Real-time PCR was performed on a Bio-Rad iQ5 Real-time PCR Detection System. Reactions were performed in a 15 μL volume in clear dome-top PCR tubes or 96-well plates with a clear adhesive cover. Control reactions contained single primer and probe combinations, while other reactions were duplexed, including an mRNA or tRNA target with 18S primers. Seven and a half microliters of iQ5 Supermix (Bio-Rad), 1 μL of each primer, probe, and template DNA were included in each reaction. In some reactions, 0.5 μL of BSA (3 μg/μL) was also added.

Reactions were optimized with primer concentrations of 0.9, 0.3, and 0.05 μM and probe concentrations of 0.25 and 0.1 μM. The optimal concentration for each oligonucleotide is presented in Table 3. In addition, a thermal gradient of 50 to 65°C was used to determine optimal annealing temperatures, which were used in subsequent experiments. Reactions were performed in duplicate, and the results were analyzed using the Bio-Rad iQ5 Optical System Software (Version 2.0). Amplification curves were analyzed as background subtracted, baseline subtracted, or baseline subtracted with a curve fit, and viewed using both logarithmic and linear scales. Thresholds were set above

background fluorescence and kept consistent for each replicate. C_T values were recorded and the amplification curves were examined. For two RNA molecules, C_T ratios were calculated and compared.

Table 3: Optimal primer and probe concentrations for each of the RNA targets.

Oligonucleotide	Concentration (μM)
β-actin forward primer	0.9
β-actin reverse primer	0.9
β-actin TaqMan® probe	0.25
Cyclophilin D forward primer	0.9
Cyclophilin D reverse primer	0.9
Cyclophilin D TaqMan® probe	0.25
GAPD forward primer	0.3
GAPD reverse primer	0.9
GAPD TaqMan® probe	0.25
$tRNA^{Ala}$ forward primer	0.9
$tRNA^{Ala}$ reverse primer	0.3
$tRNA^{Ala}$ TaqMan® probe	0.25
$tRNA^{Ser}$ forward primer	0.05
$tRNA^{Ser}$ reverse primer	0.9
$tRNA^{Ser}$ TaqMan® probe	0.25
$tRNA^{Val}$ forward primer	0.9
$tRNA^{Val}$ reverse primer	0.9
$tRNA^{Val}$ TaqMan® probe	0.25
18S forward primer	0.9
18S reverse primer	0.9
18S TaqMan® probe	0.25

RESULTS

Gel electrophoresis of control DNA PCR products showed the anticipated amplicon sizes of 178 bp for β-actin mRNA, 93 bp for cyclophilin D mRNA, 213 bp for GAPD mRNA, 85 bp for $tRNA^{Ser}$, 76 bp for $tRNA^{Val}$ and 187 bp for 18S rRNA (Figure 8). The exception was $tRNA^{Ala}$, which did not exhibit a product at the expected size of 70 bp. While a faint band was present near that location, similar bands were found in some of the other lanes and may have represented primer dimer or non-specific products.

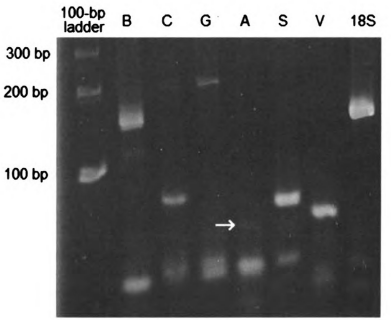

Figure 8: A 4% agarose gel displaying the control DNA PCR products. Lanes from left to right: 100-bp ladder, β-actin (B), cyclophilin D (C), GAPD (G), $tRNA^{Ala}$ (A), $tRNA^{Ser}$ (S), $tRNA^{Val}$ (V), 18S. Products of the expected sizes were visible in all lanes with the exception of $tRNA^{Ala}$. A non-specific band in that lane is indicated by an arrow.

The optimized real-time PCR protocol included a 3 minute denaturation step at 95°C, followed by 50 cycles of 95°C for 30 seconds and 55°C for 45 seconds. All targets generated a sigmoidal curve using control DNA, except $tRNA^{Ala}$ and $tRNA^{Ser}$ (Figure 9).

18S rRNA displayed the lowest C_T value, $tRNA^{Ser}$ had the highest, and $tRNA^{Ala}$ did not cross the threshold. C_T values were not affected when mRNA or tRNA genes were duplexed with the 18S gene in a separate reaction (Table 4).

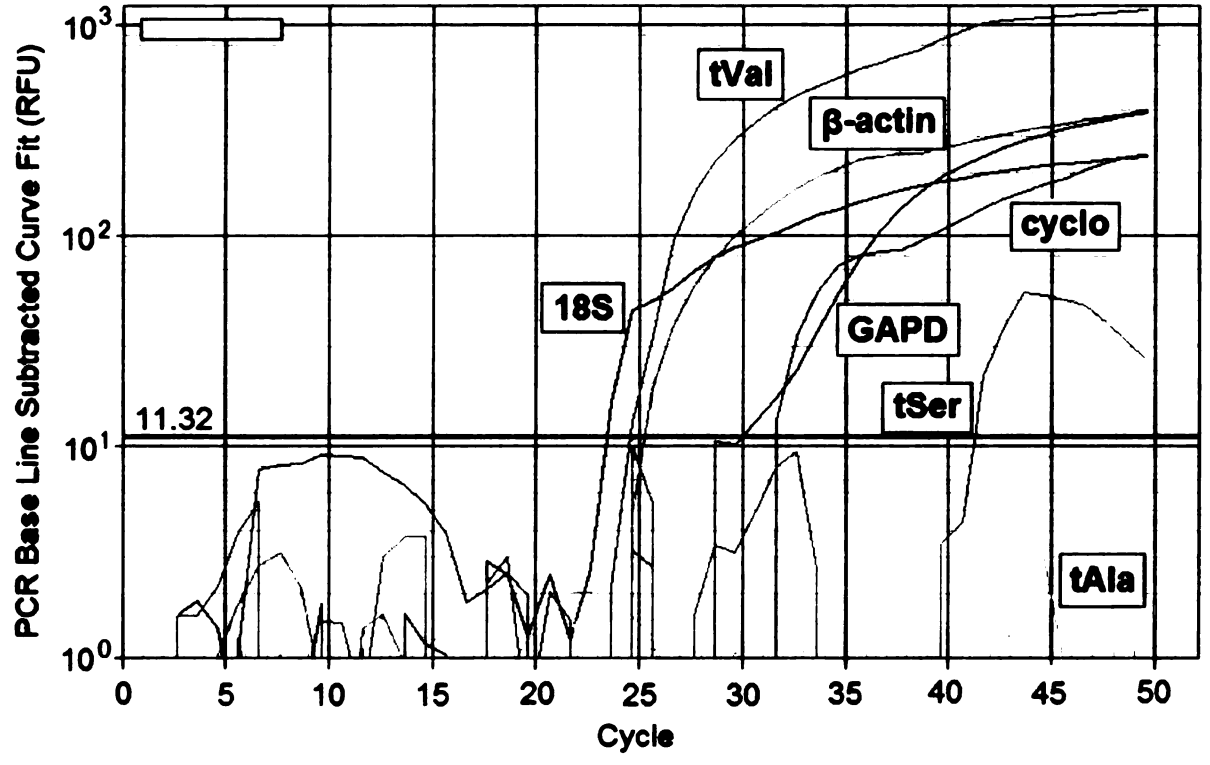

Figure 9: Logarithmic real-time amplification curves representing control DNA amplification. The threshold is shown as a bold line. The curves for 18S, β-actin, cyclophilin D (cyclo), GAPD, and $tRNA^{Val}$ (tVal) displayed a sigmoidal shape, while that for $tRNA^{Ser}$ (tSer) did not. The curve for $tRNA^{Ala}$ (tAla) did not cross the threshold.

Table 4: C_T values for each RNA target in individual and duplex reactions. The C_T value for 18S is an average, as it was included in all duplex reactions. 18S displayed the lowest C_T value, while $tRNA^{Ser}$ had the highest. The amplification curve for $tRNA^{Ala}$ did not cross the threshold and therefore a C_T value was not calculated.

Target	Individual C_T Value	Duplexed C_T Value
18S	23.28	23.62
β-actin	25.19	25.19
Cyclophilin D	31.61	32.02
GAPD	30.02	29.75
$tRNA^{Ala}$	N/A	N/A
$tRNA^{Ser}$	41.83	41.91
$tRNA^{Val}$	24.48	24.33

PCR amplification of the 10 bloodstain cDNAs ranging from 0 to 1530 days old was successful for two RNA targets (Figure 10). Reactions containing no cDNA, the reagent blank, the DNase-free control, and the controls lacking reverse transcriptase produced no product. Only 18S rRNA consistently amplified from the cDNA templates, producing bright bands for days 1510, 250, 117, 74 and 0, fainter products for days 1490 and 1440, and very weak products for days 1530 and 215. $tRNA^{Val}$ reactions from days 1530, 1490, 1425, 250 and 0 also exhibited a product of the correct size. All other RNA targets tested negative ($tRNA^{Ala}$ was not tested due to the lack of product with the DNA control).

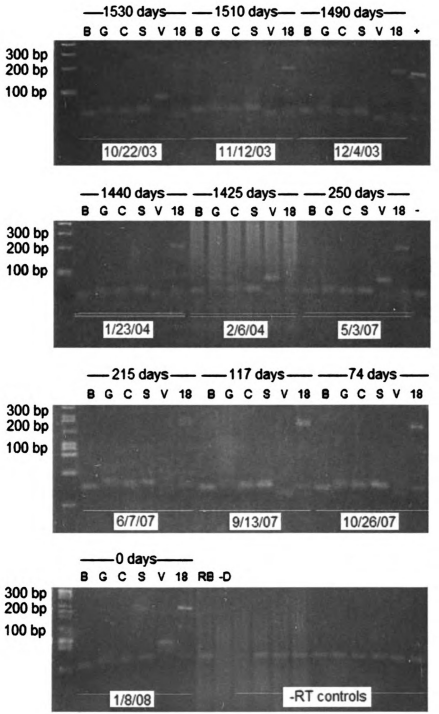

Figure 10: Multiple 4% agarose gels displaying cDNA PCR products. Dates when the bloodstains were collected are shown below the lanes. Ages of the bloodstains and the targets or controls are shown above each lane (B=β-actin, G=GAPD, C=cyclophilin D, S=$tRNA^{Ser}$, V=$tRNA^{Val}$, 18=18S, RB=reagent blank, -D=DNase-free control, -RT=reverse transcriptase-free control). All control reactions included 18S primers. 18S rRNA products were visible at all days except 1425. $tRNA^{Val}$ products were present at days 1530, 1490, 1425, 250, and 0. No products were present for any of the other RNA targets.

The results of real-time PCR using cDNAs differed somewhat from those analyzed via gel electrophoresis. cDNAs from bloodstains less than 250 days old consistently generated 18S and $tRNA^{Val}$ PCR products (Figure 11), while cDNAs from older bloodstains did not produce both products simultaneously. 18S C_T values ranged over 8.27 cycles, while those for $tRNA^{Val}$ had a range of 14.28 cycles. The average C_T value was 30.87 for 18S and 36.37 for $tRNA^{Val}$.

The C_T ratios of 18S to $tRNA^{Val}$ averaged among three or four replicates had standard deviations of less than 0.001. The ratio plot was roughly parabolic (Figure 12), remaining relatively constant at about 0.81, with 18S being more prevalent than $tRNA^{Val}$, until day 74. The relative amount of 18S had decreased by day 117, where the peak ratio was reached near 0.93. The relative concentration of $tRNA^{Val}$ had decreased at day 215, and further decreased until the ratio reached 0.84 at day 250.

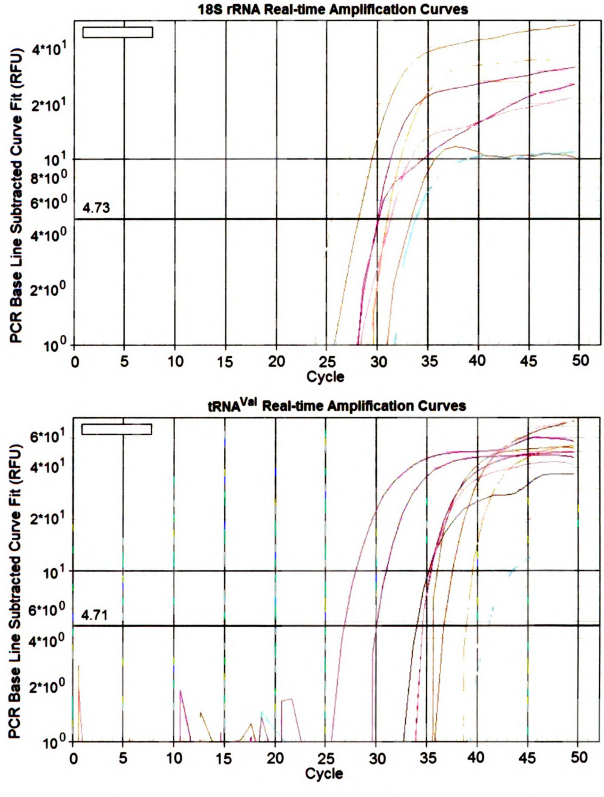

Figure 11: Logarithmic duplex real-time PCR of 18S and $tRNA^{Val}$ from bloodstain cDNAs of differing ages. Each curve displays the amplification from a single cDNA, up to the age of 250 days. The threshold is shown as a bold line. Both RNA targets amplified individually in samples older than 250 days, although not simultaneously (data not shown).

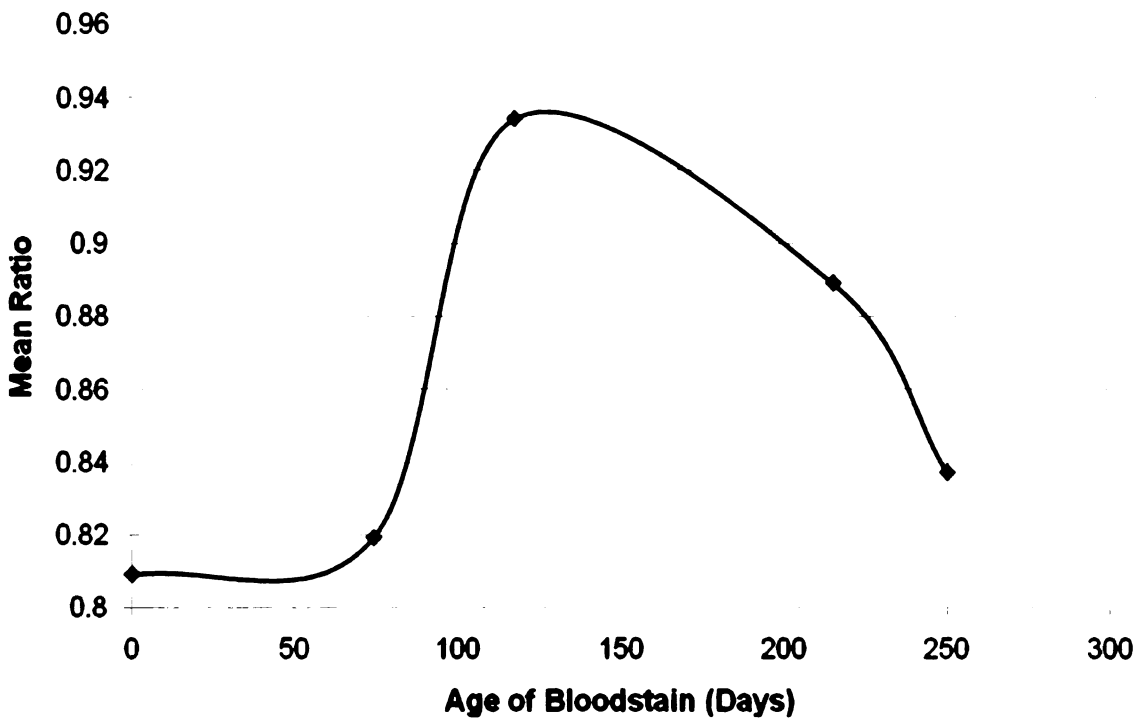

Figure 12: A curve representing the mean C_T ratio of 18S to $tRNA^{Val}$ over time. Each data point was calculated as an average of three or four replicates, producing standard deviations less than 0.001 in all cases. The curve was roughly parabolic, with a peak ratio near 0.93 occurring at 117 days. 18S was more prevalent in all of the bloodstains; however, its relative amount decreased between days 0 and 117. The relative concentration of $tRNA^{Val}$ decreased at day 215, and then further decreased until the ratio reached 0.84 at day 250.

The other duplex real-time PCRs often showed successful 18S rRNA amplification (Figure 13, region A), but the mRNA and tRNA targets did not. The real-time amplification curves for the latter RNAs were unusual, showing an increase in fluorescence beginning between cycles 15 and 20 and a subsequent decrease in fluorescence between cycles 30 and 35, resulting in a rainbow-like pattern (Figure 13, region B). In addition, several other mRNA and tRNA curves displayed an immediate increase in fluorescence that remained relatively constant throughout the thermocycling process (e.g., Figure 13, region C). Increasing the concentration of cDNA template five-

fold or decreasing it 1,000-fold produced similar results, as did varying the annealing temperature between 55 and 60°C. Also, various combinations of protocols for RNA extraction, DNase treatment, and cDNA generation did not increase amplification success. Despite using different reagents, kits, reagent volumes, and lengths of time for centrifugations and enzymatic reactions, the amplification curves for these reactions displayed a sigmoidal shape for 18S, and produced rainbows or constant fluorescence for the mRNAs and $tRNA^{Ser}$.

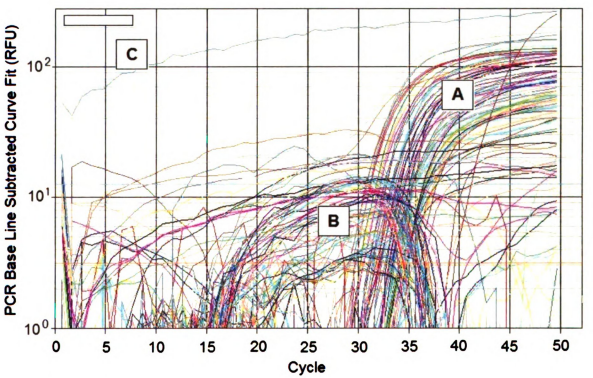

Figure 13: Logarithmic real-time PCR amplification curves for β-actin, cyclophilin D, GAPD and $tRNA^{Ser}$ duplexed with 18S. 18S amplification was sigmoidal (region A). Curves for the other RNA targets were sometimes "rainbows" (region B), which showed an increase in fluorescence followed by a decrease. Other curves displayed an immediate increase in fluorescence that remained relatively constant throughout the reaction (e.g., C).

cDNA templates from both 0.5 and 1 mL of fresh blood successfully generated 18S PCR products (Figure 14), and the average C_T value was much lower than that of the aged samples (22.13 versus 30.87). $tRNA^{Val}$ PCR product was generated using both fresh blood cDNAs, while β-actin was amplified using cDNA from the 1 mL blood sample. The β-actin amplification curve for the 0.5 mL blood sample displayed the rainbow shape described above; however, later in the reaction it also showed a sigmoidal shape similar to that generated for the 1 mL blood sample (Figure 15). The remainder of the RNA targets exhibited results similar to those for the aged bloodstains, with rainbow-shaped curves or relatively constant fluorescence.

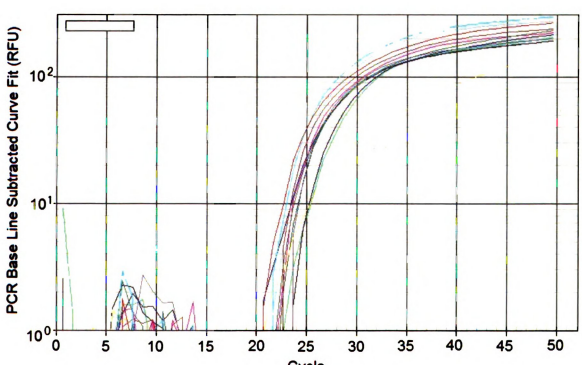

Figure 14: Logarithmic real-time PCR amplification curves for 18S rRNA using cDNA templates from 0.5 or 1 mL of fresh blood. 18S amplified from all samples when duplexed with a tRNA or mRNA target. The average C_T value among the reactions was 22.13.

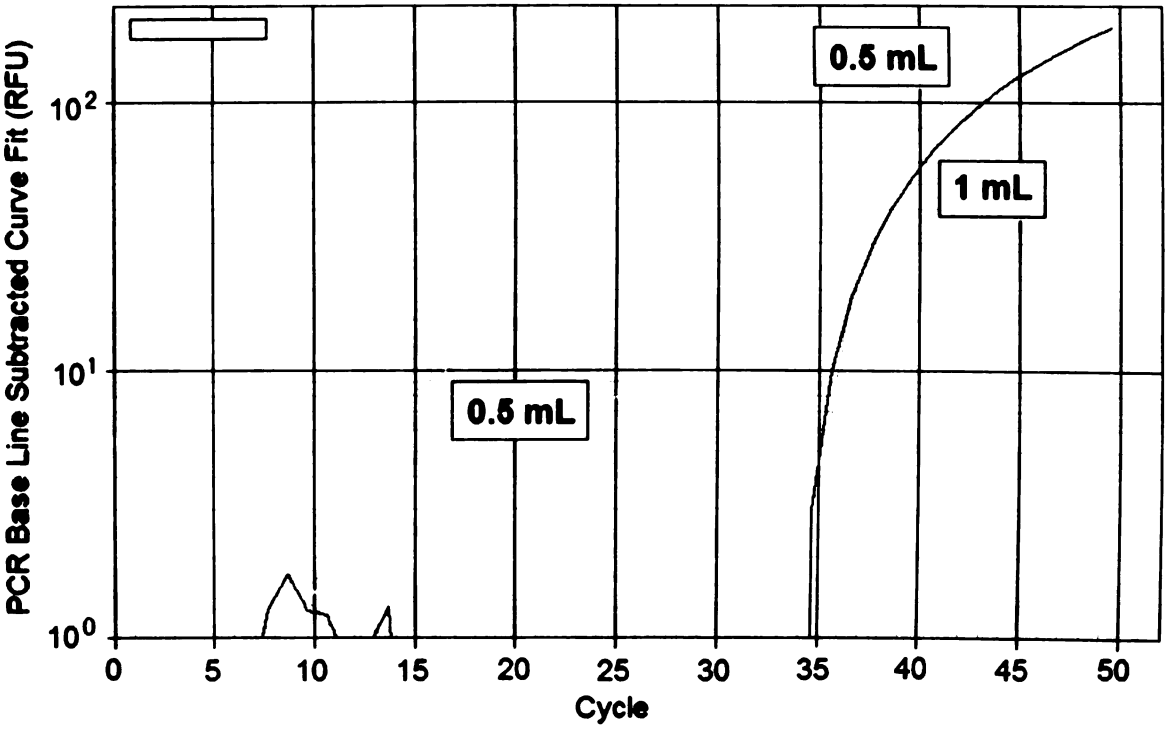

Figure 15: Logarithmic real-time PCR amplification curves for duplex β-actin and 18S using cDNA templates from 0.5 and 1 mL of fresh blood. The curve for the 0.5 mL blood sample first displayed a rainbow shape, with a subsequent sigmoidal shape occurring later in the reaction. The curve for the 1 mL sample was sigmoidal.

DISCUSSION

The aim of the research presented here was to expand on preliminary studies examining RNA degradation as a possible bloodstain aging technique. There has been little investigation into such a method, or the biological processes that are responsible for the breakdown of RNA *ex vivo*. Given this, predictions regarding degradation of different RNAs were made based on their stabilities established *in vivo*. It was hypothesized that 18S rRNA would exhibit the greatest stability over time, with tRNAs possessing moderate stability and mRNAs being the most variable and unstable. Data were obtained for two of the RNA targets, and their relationship was estimated over a period of 250 days. The remainder of the RNAs displayed negative results.

18S rRNA provided the most substantial results of all RNAs examined, as it was successfully amplified from the greatest number of aged cDNA templates. Using standard PCR, it was detected from nine of the ten bloodstains, including that aged 1530 days. 18S products were also generated in duplex with all mRNA and tRNA targets, including real-time reactions where the other target did not amplify. Previous research has characterized rRNA as relatively stable (Abelson et al., 1974), so these results were not surprising. rRNAs are also abundant; mammalian cells produce ~2 x 10^6 ribosomes per ~15 hour generation time, and 50–250 rRNA genes must be actively transcribed to meet the needs of the cell. Out of nearly 10,000 RNA species in a eukaryotic cell, rRNA consumes half of the transcriptional resources (Sollner-Webb and Tower, 1986). The 45S gene cluster that contains the 28S, 18S, and 5.8S rRNA genes is present in tandem repeats of up to 140 units spread across five different chromosomes (Stults et al., 2008). In real-time PCR studies of white blood cells, Bas et al. (2004) demonstrated that strict

regulation of rRNA production is maintained in various cellular states; levels of other RNAs fluctuated if the cells were resting or activated due to an immune response, but 18S concentration remained unchanged. The prevalence and stability of 18S likely accounts for the amplification of the rRNA in the current assay, even from bloodstains aged up to five years.

The other RNA for which positive results were obtained was $tRNA^{Val}$, which amplified from five of the ten aged cDNA templates using standard PCR, including cDNA from the 1530-day-old bloodstain. $tRNA^{Val}$ was also detected in real-time PCR using the most aged cDNA template, though it was not simultaneously amplified with 18S from templates older than 250 days. While not as abundant as 18S, $tRNA^{Val}$ has a relatively high copy number in the human genome; at least 13 genes have been discovered, including a gene cluster encoding multiple $tRNA^{Val}$ and $tRNA^{Lys}$ genes (Arnold et al., 1986; Craig et al., 1989). Also given the relative stability of tRNAs *in vivo* (Puglisi et al., 2003), the detection of $tRNA^{Val}$ from aged bloodstains was not surprising.

18S and $tRNA^{Val}$ were successfully co-amplified using cDNAs from bloodstains aged up to 250 days, so their relative degradation could be compared over time. Data were reproducible among four real-time PCR replicates from two RNA extractions, and each calculated ratio of 18S to $tRNA^{Val}$ C_T value was consistent (had a standard deviation of less than 0.001). While the limited number of data points prevented precise curve-fitting, the overall pattern indicated that degradation occurred in a variable, non-linear manner. The C_T ratio appeared relatively constant between days 0 and 74, but the lack of

interpolating data points meant that the ratio could have fluctuated. The subsequent upward trend in the curve signified that 18S was less stable than $tRNA^{Val}$. Following day 115, a negative slope was observed, indicating that the rate of decay of $tRNA^{Val}$ was greater than that of the rRNA; either $tRNA^{Val}$ degradation had increased, 18S degradation had decreased, or some combination of the two.

It seems likely that the relative degradation curve pattern resulted from fluctuations in $tRNA^{Val}$ decay, given the widely accepted stability of rRNA. Assuming this, the upward slope of the curve after day 74 meant $tRNA^{Val}$ degradation had slowed, with the subsequent downward slope caused by increased tRNA degradation. The mechanism responsible for variable $tRNA^{Val}$ degradation is unclear, though it may result from the tRNA's complex structure. The TΨC and variable loops of tRNAs are largely resistant to nucleases, while the anticodon loop and 3'-terminal CCA are most sensitive due to the tertiary structure of the molecules (reviewed by Rich and RajBhandary, 1976). 18S was likely shielded from nuclease attack owing to its location within the ribosomal complex (Merryman et al., 1999), but $tRNA^{Val}$ would have had no such protection. The tRNA was also assayed in its entirety, so any structural weaknesses were located within the amplicon. While 18S has regions of nuclease susceptibility (Matveeva et al., 1997), only 10% of the molecule was amplified, decreasing the probability that these areas were included. The exposed nature and structural sensitivity of $tRNA^{Val}$ likely accounts for the dynamic pattern of the C_T ratio curve.

Given the roughly parabolic shape of the relative degradation curve, an average C_T ratio of 0.88 (for example) corresponds to an estimated bloodstain age of either 100 or 225 days. The difference between these two dates could dramatically impact the nature of a forensic investigation. Used in conjunction with other evidence, however, it is possible that such information would be valuable. The ability to establish whether a bloodstain is relatively fresh or aged could be used to determine whether it has probative value, even if a precise temporal location could not be estimated.

It was expected that $tRNA^{Ala}$ and $tRNA^{Ser}$ would provide results similar to $tRNA^{Val}$; however, these molecules behaved very differently. $tRNA^{Ala}$ did not amplify using a DNA template, suggesting there was a problem with the primers. The spatial arrangement of the primers was similar to those of the other tRNAs, so perhaps the negative results were caused by the unique structure of the molecule. $tRNA^{Ala}$ is 70 bp in size, compared to 76 bp for $tRNA^{Val}$ and 85 bp for $tRNA^{Ser}$. It also has the highest GC content (52.8%), which should increase the strength of its secondary structure since about half of the guanines and cytosines are located within the hairpins of the tRNA. $tRNA^{Ser}$ and $tRNA^{Val}$ had similar GC percentages, at 41.2% and 40.1%, respectively. It is possible that the smaller size and more pronounced secondary structure of $tRNA^{Ala}$ was less conducive to primer binding and prevented its amplification even from a DNA template. The annealing temperature was raised incrementally up to 10°C to address this contingency, but did not lead to the generation of $tRNA^{Ala}$ PCR product. Varying the

concentration of the primers and adding BSA also did not increase the success of the reaction.

$tRNA^{Ser}$ PCR products were generated using a DNA template, but negative cDNA results were obtained from both aged and fresh bloodstains. No $tRNA^{Ser}$ products were visible on a gel following standard PCR of cDNA. In addition, real-time reactions containing $tRNA^{Ser}$ displayed rainbow-shaped amplification curves, which showed an increase in fluorescence beginning between cycles 15 and 20 and a subsequent decrease in fluorescence between cycles 30 and 35. No mention of such amplification curves was found in the literature, and inquiries with technical support from the instrument and reagent manufacturers confirmed that there had been no previous reports of similar results. It is possible that the data obtained for $tRNA^{Val}$ and $tRNA^{Ser}$ stemmed from differences in their cellular prevalence. Goh et al. (2004) surveyed 27,711 genes from 120 organisms and found that the average composition of serine and valine codons was 6.7% and 6.9%, respectively. A correlation exists between codon usage and intracellular tRNA content (Ikemura, 1982), so the corresponding tRNAs would also be maintained in equivalent concentrations. For the current study, tRNA real-time PCR probes were designed using the most prevalent human anticodons for each of the tRNAs; $tRNA^{Val}$(CAC;48.5%), $tRNA^{Ala}$ (GGC;41.5%), and $tRNA^{Ser}$(GCU;25.5%) (Ikemura, 1985). This still does not explain the successful amplification of only $tRNA^{Val}$, though, since the variability in initial tRNA concentration would reflect a difference of less than one PCR cycle. Although $tRNA^{Ser}$ was present in half the initial quantity of $tRNA^{Val}$,

$tRNA^{Ser}$ PCR product should have been generated if its cDNA was present in the reaction.

Cellular modifications may have also impacted tRNAs differently. tRNAs are extensively altered in order to promote efficiency of protein production (Yarian et al., 2002), including methylation, adenylation, ubiquitination, and atom exchange (e.g., sulfur for oxygen), among many others (Nakai et al., 2008). Modifications can also involve complex sequential reactions that result in formation of unique nucleosides, such as queuosine or inosine (Björk et al., 1987). While modifications of tRNA occur normally, they can increase when cells undergo a change in environment. Wust and Rosen (1972) demonstrated that tRNA in younger rats was more methylated than that from older rats. In addition, studies of monkey kidney epithelial cells experiencing methionine starvation showed that phenylalanine tRNAs lacked the wye base, a derivative of guanosine normally present in eukaryotic cells (Pergolizzi et al., 1978). No studies involving the impact of these altered bases on PCR amplification were found in the literature. It is possible that $tRNA^{Ser}$ possessed a greater number of modifications than $tRNA^{Val}$, or that $tRNA^{Ser}$ contained a specific modified nucleoside that hindered primer binding during reverse transcription. This would have prevented creation of the cDNA and account for its lack of real-time PCR detection. Otherwise, the structures of the tRNAs near the ends of the molecules are similar and should not have caused differential primer binding.

The housekeeping mRNAs β-actin, cyclophilin D, and GAPD were all successfully amplified using DNA templates, but displayed negative results from cDNA templates. It is likely that the rainbow real-time amplification curves obtained for these RNAs were caused by a technical problem, since researchers routinely use real-time PCR to quantify

mRNA levels in blood. Dheda et al. (2004) compared β-actin, cyclophilin, and GAPD as internal standards for gene expression in whole blood and peripheral blood mononuclear cell cultures and found that all had C_T values of less than 30. In addition, Raghavan et al. (2002) used real-time PCR to confirm results from microarray gene expression analysis in white blood cells and demonstrated that mRNA half-lives obtained using both methods were well-correlated. Data from the microarrays indicated that the majority of the mRNAs had half-lives greater than 6 hours, and that many were selectively stabilized or degraded following lymphocyte activation. These studies used large quantities of RNA for cDNA synthesis; Dheda et al. (2004) isolated up to 5 μg from 2.5 mL of whole blood, and Raghavan et al. (2002) extracted 10–15 μg from cultured lymphocytes. Anderson et al. (2005) demonstrated success with much smaller quantities of RNA; β-actin was amplified using RNA isolated from less than 1 μL of fresh blood. In the current study, the aged bloodstains were approximately 10 μL in volume and dried onto a petri dish, so it is reasonable to suggest that RNA purification from these samples was more difficult. However, the use of large volumes of fresh blood still resulted in the rainbow amplification curves for cyclophilin and GAPD mRNAs.

One mRNA in the current study did amplify using large volumes of blood; β-actin cDNA from the 0.5 mL blood sample produced a rainbow amplification followed by a standard sigmoidal curve, while the 1 mL sample produced a normal curve. These results indicate that initial cDNA concentrations impacted the shape of the amplification curve, and that the rainbow curve was associated with smaller starting amounts of cDNA. Because cDNA from the 1 mL blood sample was twice as concentrated as that from the 0.5 mL sample, the difference between them should have been one PCR cycle. The C_T

values for each reaction were even closer than this: 35.92 for the 0.5 mL sample and 35.63 for the 1 mL sample. Therefore, the initial increase in fluorescence observed between cycles 15 and 20 did not likely represent creation of PCR product. Additionally, the C_T values associated with the rainbow curves were lower than the 18S C_T values for the 0.5 and 1 mL blood samples, and it is improbable that less-prevalent targets from aged templates would have been present at higher concentrations than the rRNA. The subsequent decrease in fluorescence is also unlikely to represent the loss of product during the thermocycling process, since DNA routinely withstands denaturation. The fact that positive mRNA results were only obtained using such a large initial volume of blood suggests that there may have been a problem with the quality of the RNA. It is possible that mRNAs were experiencing rapid degradation immediately following RNA purification, and that β-actin was only present in detectable quantities in the 1 mL sample prior to cDNA synthesis. This explanation is unconvincing, since RNA extraction methods require less time than is average for an mRNA half-life (Sharova et al., 2009). If exogenous RNase activity were to blame, it would be expected that the other RNAs would be affected, but both 18S and $tRNA^{Val}$ displayed positive results for the fresh blood samples. The differences in C_T values for 18S and $tRNA^{Val}$ using the large volumes of blood were consistent with the results attained from the aged bloodstain cDNAs; average C_T values for the aged cDNAs were 30.87 for 18S and 36.37 for $tRNA^{Val}$, while those for the fresh blood samples were 22.13 for 18S and 30.42 for $tRNA^{Val}$.

The amplification of 18S and $tRNA^{Val}$ from both fresh and aged blood templates indicates that RNA was present in sufficient quantities for reverse transcription following purification and suggests that the negative results obtained for the other RNAs resulted from problems during this process. There are three mechanisms by which cDNAs can be generated: random priming, oligo-dT priming, or target-specific priming (reviewed by Bustin and Nolan, 2004). Target-specific priming is the most sensitive, but is time-consuming since separate reverse transcription reactions must be carried out for each RNA target. In addition, it requires larger amounts of starting RNA, less than ideal in a forensic setting. Oligo-dT priming is specific to mRNA as the primers anneal to the poly(A) tail; therefore, it was not viable in this study. Random primers anneal to RNA in multiple locations and create cDNAs of varying lengths, which can misrepresent cDNA copy numbers (Zhang and Byrne, 1999). However, random primers are best for targets with strong secondary structure (reviewed by Bustin and Nolan, 2004), which was important in the current study given tRNAs and rRNA were assayed. Those authors stated that the majority of cDNA synthesized from total RNA using random primers come from rRNA, and proposed the potential for inefficient priming of less-prevalent RNAs. The relative abundance of 18S might have out-competed cDNA priming of lower-copy targets and led to the unsuccessful results for the other RNAs in the research presented here. If this were true, the positive results attained using $tRNA^{Val}$ suggest that it was the only other RNA present in sufficient quantities to be primed and copied into cDNA. This explanation is most plausible for the aged bloodstains, since degradation of the mRNAs would cause them to be more under-represented in the RNA extracts.

However, it still does not satisfactorily account for the negative results obtained using fresh blood.

Other technical factors that could have resulted in the unexpected amplification curves were errors in the real-time PCR detection system and its analysis of the fluorescence generated during the reactions. The curves were examined using multiple modes of analysis, but even the raw data exhibited patterns similar to the curves when viewed with a logarithmic scale. Calibration errors were ruled out as a possible cause of the negative results, since all dyes were detected in real-time reactions using DNA as a template. Additionally, other researchers in the laboratory have used the same instrument, calibration methods, and dyes, without experiencing rainbow amplification curves.

CONCLUSIONS

The ability to link deposition of a bodily fluid to a point in time would greatly benefit a criminal investigation. Unfortunately, the results of the current study indicate there are pitfalls associated with the analysis of RNA degradation in aged bloodstains. The method as presented here could not be used to age biological evidence collected from a crime scene. However, the most plausible explanation for the negative results is a technical problem, which may be overcome through further investigation. Rainbow amplification curves were obtained from fresh blood as well as aged samples, showing that those results were not related to sample age. The mRNAs and $tRNA^{Ser}$ may have been out-competed by 18S, so inclusion of less-prevalent targets might establish a more dynamic range for real-time PCR. Such targets could include small nuclear RNAs (snRNAs), which process pre-mRNA (Krämer, 1996), ribonuclease MRP RNAs, which cleave rRNA precursors (López et al., 2009), or precursor tRNAs, which contain introns

in extended anticodon loops (Swerdlow and Guthrie, 1984). These non-coding RNAs have unique secondary structures and likely possess intermediate stabilities, lacking the decay elements present in mRNAs or the protein protection provided rRNAs (Guhaniyogi and Brewer, 2001; Merryman et al., 1999). Genome copy-number bias could also be eliminated through concurrent DNA analysis. Real-time PCR amplification of cDNA could be normalized to amplification of the corresponding DNA, with cDNA primers spanning intron-exon boundaries and preventing DNA amplification.

Despite the problems encountered during this study, two of the RNAs displayed positive results using aged bloodstain cDNAs, meaning it is possible to detect RNA from samples aged up to five years. The fluctuating degradation pattern observed for 18S and $tRNA^{Val}$ could limit its forensic applicability, but was based on data gathered from a limited number of aged bloodstains. An analysis of samples collected more frequently over a longer period of time could establish whether a more predictable pattern of degradation between these two markers exists. Even if a precise time of stain deposition could not be ascertained, an aging method based on RNA degradation may be used to establish whether a biological stain has probative value. This could aid investigators in determining whether a location was the scene of a crime, or if a biological stain should undergo further DNA analysis.

REFERENCES

Abelson, H.T., Johnson, L.F., Penman, S. and Green, H. 1974. Changes in RNA in relation to growth of the fibroblast. II. The lifetime of mRNA, rRNA and tRNA in resting and growing cells. *Cell* 1:161–165.

ABI PRISM 7700 (TaqMan® assay) Amplification Curve. 2009. Cosmo Bio Co., Ltd. website. Available at <http://www.cosmobio.co.jp/export_e/products/molecular/products_TYB_20060907.asp>.

Achsel, T. and Gross, H.J. 1993. Identity determinants of human $tRNA^{Ser}$: sequence elements necessary for serylation and maturation of a tRNA with a long extra arm. *EMBO Journal* 12: 3333–3338.

Alexandrov, A., Chernyakov, I., Gu, W., Hiley, S.L., Hughes, T.R., Grayhack, E.J. and Phizicky, E.M. 2006. Rapid tRNA decay can result from lack of nonessential modifications. *Molecular Cell* 21: 87–96.

Anderson, S., Howard, B, Hobbs, G. and Bishop, C. 2005. A method for determining the age of a bloodstain. *Forensic Science International* 148: 37–45.

Arnold, G.J., Schmutzler, C., Thomann, U., Van Tol, H. and Gross, H.J. 1986. The human $tRNA^{Val}$ gene family: organization, nucleotide sequences and homologous transcription of three single-copy genes. *Gene* 44(2): 287-297.

Bas, A., Forsberg, G., Hammarstrom, S. and Hammarstrom, M.L. 2004. Utility of the housekeeping genes 18S, β-actin and glyceraldehyde-3-phosphate dehydrogenase for normalization in real-time quantitative reverse transcriptase-polymerase chain reaction analysis of gene expression in human T lymphocytes. *Scandinavian Journal of Immunology* 59(6): 566–573.

Bauer, M., Polzin, S. and Patzelt, D. 2003. Quantification of RNA degradation by semi-quantitative duplex and competitive RT-PCR: a possible indicator of the age of bloodstains? *Forensic Science International* 138: 94–103.

Björk, G.R., Ericson, J.U., Gustafsson, C.E.D., Hagervall, T.G., Jönsson, Y.H. and Wikström, M. 1987. Transfer RNA modification. Annual Review of Biochemistry 56: 263–287.

Bloch, W. 1991. A biochemical perspective of the polymerase chain reaction. *Biochemistry* 30: 2735–2747.

Bolognani, F. and Perrone-Bizzozero, N.I. 2008. RNA-protein interactions and control of mRNA stability in neurons. *Journal of Neuroscience Research* 86: 481–489.

Bustin, S.A. and Nolan, T. 2004. Pitfalls of quantitative real-time reverse-transcription polymerase chain reaction. *Journal of Biomolecular Techniques* 15: 155–166.

Carraro, G., Albertin, G., Forneris, M. and Nussdorfer, G.G. 2005. Similar sequence-free amplification of human glyceraldehyde-3-phosphate dehydrogenase for real time RT-PCR applications. *Molecular and Cellular Probes* 19(3): 181–186.

Craig, L.C., Wang, L.P., Lee, M.M., Pirtle, I.L. and Pirtle, L.M. 1989. A human tRNA gene cluster encoding the major and minor valine tRNAs and a lysine tRNA. *DNA* 8:457-471.

Davis, A. 2005. Cells 101: Business Basics. In: Inside the Cell. National Institutes of Health publication. Available at <http://publications.nigms.nih.gov/insidethecell/pdf/inside_the_cell.pdf>.

de Pouplana, L.R. and Schimmel, P. 2001. Operational RNA code for amino acids in relation to genetic code in evolution. *Journal of Biological Chemistry* 276(10): 6881–6884.

Deshmukh, M., Tsay, Y., Paulovich, A.G. and Woolford, J.L. 1993. Yeast ribosomal protein L1 is required for the stability of newly synthesized 5S rRNA and the assembly of 60S ribosomal subunits. *Molecular and Cellular Biology* 13(5): 2835–2845.

Dheda, K., Huggett, J.F., Bustin, S.A., Johnson, M.A., Rook, G. and Zumla, A. 2004. Validation of housekeeping genes for normalizing RNA expression in real-time PCR. *Biotechniques* 37(1): 112–117.

Eck, J., Chainey, S., Cameron, J., Leitner, M. and Wilson, R. 2005. Mapping crime: Understanding hot spots. U.S. National Institute of Justice Special Report.

Engelke, D.R. and Hopper, A.K. 2006. Modified view of tRNA: stability amid sequence diversity. *Molecular Cell* 21: 144–145.

Foran, D.R., Gehring, M.E., and Stallworth, S.E. 2009. The recovery and analysis of mitochondrial DNA from exploded pipe bombs. *Journal of Forensic Sciences* 54(1): 90–94.

Goh, C., Lan, N., Douglas, S.M., Wu, B., Echols, N., Smith, A., Milburn, D., Montelione, G.T., Zhao, H. and Gerstein, M. 2004. Mining the structural genomics pipeline: identification of protein properties that affect high through-put experimental analysis. *Journal of Molecular Biology* 336: 115–130.

Gowrishankar, G., Winzen, R., Bollig, F., Ghebremedhin, B., Redich, N., Ritter, B., Resch, K., Kracht, M. and Holtmann, H. 2005. Inhibition of mRNA deadenylation and degradation by ultraviolet light. *Biological Chemistry* 386(12): 1287–1293.

Graifer, D., Molotkov, M., Styazhkina, V., Demeshkina, N., Bulygin, K., Eremina, A., Ivanov, A., Laletina, E., Ven'yaminova, A. and Karpova, G. 2004. Variable and conserved elements of human ribosomes surrounding the mRNA at the decoding and upstream sites. *Nucleic Acids Research* 32(11): 3282–3293.

Greatrix, B.W. and van Vuuren, H.J. 2006. Expression of the HXT13, HXT15 and HXT17 genes in Saccharomyces cerevisiae and stabilization of the HXT1 gene transcript by sugar-induced osmotic stress. *Current Genetics* 49: 205–217.

Guhaniyogi, J. and Brewer, G. 2001. Regulation of mRNA stability in mammalian cells. *Gene* 265(1–2): 11–23.

Heid, C.A., Stevens, J., Livak, K.J. and Williams, P.M. 1996. Real time quantitative PCR. *Genome Research* 6: 986–994.

Herruer, M.H., Mager, W.H., Raué, H.A., Verken, P., Wilms, E. and Planta, R.J. 1988. Mild temperature shock affects transcription of yeast ribosomal protein genes as well as the stability of their mRNAs. *Nucleic Acids Research* 16(16): 7917–7929.

Hofreiter, M., Serre, D., Poinar, H., Kuch, M., and Pääbo, S. 2001. Ancient DNA. *Nature* 2: 353–359.

Holland, P.M., Abramson, R.D., Watson, R. and Gelfand, D.H. 1991. Detection of specific polymerase chain reaction product by utilizing the 5'-3' exonuclease activity of Thermus aquaticus DNA polymerase. *Proceedings of the National Academy of Sciences* 88: 7276–7280.

Houseley, J. and Tollervey, D. 2009. The many pathways of RNA degradation. *Cell* 136(4): 763–776.

Ikemura, T. 1982. Correlation between the abundance of yeast transfer RNAs and the occurrence of the respective codons in protein genes. *Journal of Molecular Biology* 158: 573–597.

Ikemura, T. 1985. Codon usage and tRNA content in unicellular and multicellular organisms. *Molecular Biology and Evolution* 2:13–34.

Johnson, L.F., Abelson, H.T., Green, H. and Penman, S. 1974. Changes in RNA in relation to growth of the fibroblast. I. Amounts of mRNA, rRNA, and tRNA in resting and growing cells. *Cell* 1: 95–100.

Jona, G., Choder, M. and Gileadi, O. 2000. Glucose starvation induces a drastic reduction in the rates of both transcription and degradation of mRNA in yeast. *Biochimica et Biophysica Acta* 1491: 37–48.

Kadaba, S., Krueger, A., Trice, T., Krecic, A.M., Hinnebusch, A.G. and Anderson, J. 2004. *Genes & Development* 18: 1227–1240.

Kobilinsky, L. 1992. Recovery and stability of DNA in samples of forensic science significance. *Forensic Science Review* 4: 67–87.

Krämer, A. 1996. The structure and function of proteins involved in mammalian pre-mRNA splicing. *Annual Review of Biochemistry* 65: 367–409.

López, M.D., Rosenblad, M.A and Samuelsson, T. 2009. Conserved and variable domains of RNase MRP RNA. *RNA Biology* 6(3): 209–220.

Mathews, C., Van Holde, K.E. and Ahern, K. 2000. Biochemistry. 3rd Edition. San Francisco: Addison Wesley Longman.

Matveeva, O., Felden, B., Audlin, S., Gesteland, R.F. and Atkins, J.F. 1997. A rapid *in vitro* method for obtaining RNA accessibility patterns for complementary DNA probes: correlation with an intracellular pattern and known RNA structures. *Nucleic Acids Research* 25(24): 5010–5016.

Medhurst, A.D., Harrison, D.C., Read, S.J., Campbell, C.A., Robbins, M.J. and Pangalos, M.N. 2000. The use of TaqMan RT-PCR assays for semiquantitative analysis of gene expression in CNS tissues and disease models. *Journal of Neuroscience Methods* 98(1): 9–20.

Merryman, C., Moazed, D., Daubresse, G. and Noller, H.F. 1999. Nucleotides in 23S rRNA protected by the association of 30S and 50S ribosomal subunits. *Journal of Molecular Biology* 285(1): 107–113.

Morse, D.L., Carroll, D., Weberg, L., Borgstrom, M.C., Ranger-Moore, J. and Gillies, R.J. 2005. Determining suitable internal standards for mRNA quantification of increasing cancer progression in human breast cells by real-time reverse transcriptase polymerase chain reaction. *Analytical Biochemistry* 342(1): 69–77.

Nakai, Y., Nakai, M. and Hayashi, H. 2008. Thio-modification of yeast cytosolic tRNA requires a ubiquitin-related system that resembles bacterial sulfur transfer systems. *Journal of Biological Chemistry* 283(41): 27469–27476.

Niki, T., Iba, S., Tokunou, M., Yamada, T., Matsuno, Y. and Hirohashi, S. 2000. Expression of vascular endothelial growth factors A, B, C, and D and their relationships to lymph node status in lung adenocarcinoma. *Clinical Cancer Research* 6: 2431–2439.

Noller, H.F. 1991. Ribosomal RNA and translation. *Annual Review of Biochemistry* 60: 191–227.

Ochberg, F. 2002. A primer on interviewing victims. In Simple and Complex Post-Traumatic Stress Disorder: Strategies for Comprehensive Treatment in Clinical Practice. Edited by M. Williams and J. Sommer Jr. Haworth Press: 351–357.

Pergolizzi, R.G., Engelhardt, D.T. and Grunberger, D. 1978. Formation of phenylalanine tRNA lacking the Wye base in Vero cells during methionine starvation. *Journal of Biological Chemistry* 253: 6341–6343.

Puglisi, J.D., Pütz, J., Florentz, C. and Giegé, R. 1993. Influence of tRNA tertiary structure and stability on aminoacylation by yeast aspartyl-tRNA synthetase. *Nucleic Acids Research* 21(1): 41–49.

Raghavan, A., Ogilvie, R.L., Reilly, C., Abelson, M.L., Raghavan, S., Vasdewani, J., Krathwohl, M. and Bohjanen, P.R. 2002. Genome-wide analysis of mRNA decay in resting and activated primary human T lymphocytes. *Nucleic Acids Research* 30(24): 5529–5538.

Ratcliffe, J. 2002. Aoristic signatures and the spatio-temporal analysis of high volume crime patterns. *Journal of Quantitative Criminology* 18(1): 23–43.

Rich, A. and RajBhandary, U.L. 1976. Transfer RNA: Molecular structure, sequence, and properties. *Annual Review of Biochemistry* 45: 805–860.

Sahmi, M., Nicola, E.S. and Price, C.A. 2006. Hormonal regulation of cytochrome P450 aromatase mRNA stability in non-luteinizing bovine granulosa cells *in vitro*. *Journal of Endocrinology* 190: 107–115.

Saiki R.K., Gelfand D.H., Stoffel S., Scharf S.J., Higuchi R., Horn G.T., Mullis K.B. and Erlich H.A. 1988. Primer-directed enzymatic amplification of DNA with a thermostable DNA polymerase. *Science* 239:487–491.

Schlegel, R.A., Iversen, P. and Rechsteiner, M. 1978. The turnover of tRNAs microinjected into animal cells. *Nucleic Acids Research* 5(10): 3715–3729.

Sharova, L.V., Sharov, A.A., Nedorezov, T., Piao, Y., Shaik, N. and Ko, M.S.H. 2009. Database for mRNA half-life of 19,977 genes obtained by DNA microarray analysis of pluripotent and differentiating mouse embryonic stem cells. *DNA Research* 16: 45–58.

Sollner-Webb, B. and Tower, J. 1986. Transcription of cloned eukaryotic ribosomal RNA genes. *Annual Review of Biochemistry* 55: 801–830.

Stults, D.M., Killen, M.W., Pierce, H.H. and Pierce, A.J. 2008. Genomic architecture and inheritance of human ribosomal RNA gene clusters. *Genome Research* 18:13-18.

Swerdlow, H. and Guthrie, C. 1984. Structure of intron-containing tRNA precursors. *The Journal of Biological Chemistry* 259(8): 5197–5207.

TaqMan® Gene Expression Assays for Validating Hits from Fluorescent Microarrays. 2006. Applied Biosystems White Paper TaqMan® Gene Expression Assays document. Available at <http://www3.appliedbiosystems.com/cms/groups/mcb_marketing/documents/generaldocuments/cms_040198.pdf>.

Tarone, A., Jennings, K. and Foran, D. 2007. Aging blow fly eggs using gene expression: a feasibility study. *Journal of Forensic Sciences* 52(6): 1350–1354.

Temin, H.M. and Mizutani, S. 1970. Viral RNA-dependent DNA polymerase: RNA-dependent DNA polymerase in virions of Rous Sarcoma Virus. *Nature* 226: 1211–1213.

Wang, S. and Kool, E.T. 1995. Origins of the large differences in stability of DNA and RNA helices: C-5 methyl and 2'-hydroxyl effects. *Biochemistry* 34(12): 4125–4132.

Weedn, V.W. and Roby, R.K. 1993. Forensic DNA Testing. *Archives of Pathology and Laboratory Medicine* 117(5): 486–491.

Wickenheiser, R. 2002. Trace DNA: A review, discussion of theory, and application of the transfer of trace quantities of DNA through skin contact. *Journal of Forensic Sciences* 47: 442–450.

Wilusz, C.J., Wormington, M., and Peltz, S.W. 2001. The cap-to-tail guide to mRNA turnover. *Nature Reviews Molecular Cell Biology* 2: 237–246.

Wust, C.J. and Rosen, L. 1972. Aminoacylation and methylation of tRNA as a function of age in the rat. *Experimental Gerontology* 7: 335–343.

Yarian, C., Townsend, H., Czestkowski, W., Sochacka, E., Malkiewicz, A., Guenther, R., Miskiewicz, A. and Agris, P. 2002. Accurate translation of the genetic code depends on tRNA modified nucleosides. *Journal of Biological Chemistry* 277(19): 16391–16395.

Zhang, J. and Byrne, C.D. 1999. Differential priming of RNA templates during cDNA synthesis markedly affects both accuracy and reproducibility of quantitative competitive reverse transcriptase PCR. *Biochemical Journal* 337: 231–241.

Zimmermann, K. and Mannhalter, J.W. 1996. Technical aspects of quantitative competitive PCR. *Biotechniques* 21(2): 268-272, 274–279.